Biomedicine & Pharmacotherapy 194 (2026) 118961

Contents lists available at ScienceDirect

Biomedicine & Pharmacotherapy

journal homepage: www.elsevier.com/locate/biopha

Extracellular vesicles from microalgae as natural bioactive agents for UVB protection, anti-aging, and skin depigmentation

Paola Gargano [a,b,c,1], Sabrina Picciotto [a,b,1], Angela Paterna [b], Samuele Raccosta [b], Estella Rao [b], Daniele Paolo Romancino [a], Giulia Smeraldi [a], Mauro Manno [b,c], Monica Salamone [a], Natasa Zarovni [a,c], Giorgia Adamo [a], Antonella Bongiovanni [a,c,*]

[a] Cell-Tech HUB and Institute for Research and Biomedical Innovation (IRIB), National Research Council of Italy (CNR), Palermo 90146, Italy
[b] Cell-Tech HUB and Institute of Biophysics (IBF) - National Research Council of Italy (CNR), Palermo 90146, Italy
[c] EVEBiofactory at Cell-Tech HUB, National Research Council of Italy (CNR), Palermo 90146, Italy

ARTICLE INFO

Dataset link: research data_gargano

Keywords:
Microalgae-derived extracellular vesicles
Exosomes
Nanoalgosomes
Skin photoprotection
UVB-induced damage
Dermocosmetic ingredients
Melanogenesis modulation

ABSTRACT

The search for effective dermocosmetic treatments has recently been accompanied by the growing demand for ingredients that are both naturally derived and sustainable. In this context, microalgae have emerged as a promising biofactory, producing bioactive compounds for skin health, widely recognized for their antioxidant, anti-inflammatory, and anti-aging activities. To leverage these properties, beyond the conventional use of microalgal biomass or extracts, the isolation and application of their secretome, including the extracellular vesicles named "nanoalgosomes", emerged as a novel approach. Extracellular vesicles are membranous nanoparticles released by all cells and naturally efficient in the transport of both endogenous and exogenous bioactive molecules. Their unique biological properties make them ideal candidates for therapeutic and cosmetic applications. Here, we propose nanoalgosomes, as a sustainable and effective solution for innovative dermocosmetic treatments. In this study we exemplify the use of the microalgae *Tetraselmis chuii,* an edible, green and renewable bio-source of extracellular vesicles. We demonstrated the nanoalgosomes' skin-health promoting potential, by employing the human skin cells as model to evidence the nanoalgosome ability to protect the cells from ultraviolet B (UVB) radiation-related damages, by reducing both the oxidative stress, and senescence-associated phenotype in UVB-exposed skin cells. Furthermore, nanoalgosomes modulate melanogenesis in UVB-stimulated melanocytes by downregulating tyrosinase, significantly reducing melanin content, supporting their role as photoprotective and pigmentation-modulating agents. Altogether, our results provide a solid foundation for the development of nanoalgosome-based formulations in dermocosmetic applications aimed at UV protection, anti-aging, and depigmentation, supporting the transition toward natural and sustainable skincare solutions.

1. Introduction

The dermocosmetic industry has been significantly influenced by the growing demand for eco-friendly products, driving a shift toward the use of natural and sustainable ingredients. While natural compounds are often perceived as safer and more effective for skin health, their large-scale use presents significant environmental challenges, including extensive water consumption, land exploitation, and biodiversity depletion. Additionally, natural extracts often suffer from variability in composition due to differences in cultivation methods, climate conditions, and extraction processes, raising concerns about their standardization.

To overcome these limitations, innovative bio-based approaches from cellular biotechnology are bridging sustainability and performance. One of the most promising approaches in this field is the use of extracellular vesicles (EVs) as innovative carriers for bioactive molecules in both therapeutic and cosmetic applications. EVs are nanosized lipid-bilayer delimited vesicles physiologically released by all cell types,

* Corresponding author at: Cell-Tech HUB and Institute for Research and Biomedical Innovation (IRIB), National Research Council of Italy (CNR), Palermo 90146, Italy.
E-mail address: antonella.bongiovanni@cnr.it (A. Bongiovanni).
[1] These Authors contributed equally to this work and shared the first authorship.

https://doi.org/10.1016/j.biopha.2025.118961
Received 31 October 2025; Received in revised form 19 December 2025; Accepted 27 December 2025
Available online 6 January 2026
0753-3322/© 2025 The Authors. Published by Elsevier Masson SAS. This is an open access article under the CC BY-NC-ND license (http://creativecommons.org/licenses/by-nc-nd/4.0/).

playing a crucial role in cell-to-cell communication by transporting biomolecules, at most represented by proteins, lipids, and nucleic acids [1,2]. In recent years, EV-based formulations emerged as alternative to traditional synthetic lipid-based systems, such as liposomes and lipid nanoparticles [3–5]. While liposomes have been widely used in cosmetic formulations due to their ability to encapsulate and deliver active ingredients, they lack the intrinsic biological functionality of EVs [6]. Additionally, EVs have been shown to improve stability and protection for encapsulated compounds, making them highly attractive for the management of skin-related disorders and dysfunctions. Despite these advantages, mammalian-derived EVs face challenges related to large-scale production, standardization and safety, and are currently prohibited in Europe and China for the cosmetic application. To find more sustainable and scalable EV sources, researchers have turned to alternatives, one of which is remarkably presented by microalgae. Microalgae are photosynthetic microorganisms, rich in valuable metabolites, including antioxidants, polysaccharides, peptides, and pigments, some of which have been shown to exert beneficial effects for skin health. For that reason, microalgae have gained increasing attention as a sustainable and versatile source of bioactive compounds for cosmetics. Nanoalgosomes (ALG) are microalgae-derived small extracellular vesicles that share fundamental properties with small EVs (including exosomes), such as nanoscale size, membrane-bound structure, specific EV biomarkers, and the ability to be internalized by various human cells. Importantly, nanoalgosomes shown to be highly stable in biological fluids, an additional feature to confirm their promising potential for applications in the cosmetic and pharmaceutic industry [7,8]. In this study, we investigated the potential of *Tetraselmis chuii*-derived nanoalgosomes (*TC*-ALG) as an innovative, biocompatible, sustainable and bio-active nanocarriers for skin health. The premises of the current study were built upon our previous studies that demonstrated that *TC*-ALG exhibit pronounced antioxidant and anti-inflammatory properties, as well as an *in vivo* biocompatibility [7,9,10].

Human skin is an organ that has many roles like thermoregulation and regulation of hydration, while it especially works as a barrier to protect from external factors such as mechanical stress, infection and UV radiations [11,12]. The natural defence against UV rays is exerted by a specific type of cells situated in the epidermis, the melanocytes. When stimulated by UV rays, they produce melanin, which is then transferred to keratinocytes and works like a natural sunscreen [13,14]. There are three different types of UV rays: UVC, that are the most dangerous, typically shielded by ozone; UVA (320–400 nm) that can reach the dermis and cause redness, furrows, aging and melanoma; and UVB (280–320 nm) that affect the epidermis, determining tan, but can also cause cell damage and tumours [13,15–17]. Prolonged exposure to UV rays results in the rise of intracellular reactive oxygen species (ROS) and the activation of inflammatory and apoptotic pathways [18,19]. These molecular events promote the accumulation of senescent cells, characterized by increased senescence-associated (SA)-β-galactosidase activity and secretion of pro-inflammatory mediators [20]. From a more strictly dermocosmetic perspective these events can also lead to age-related skin issues such as dark spots, wrinkles, and loss of elasticity. Overall, all these events are responsible for the phenomenon known as photoaging [21,22].

In this context, recent evidence demonstrated that EVs (*e.g.* exosomes) derived from human stem cells can counteract senescence in fibroblasts, reduce matrix metalloproteinases expression, enhance collagen synthesis, and restore extracellular matrix homeostasis [20]. Among the various active ingredients, marine microalgae chemical extract has also been shown to possess photoprotective activity, improving cell viability, rebalancing the oxidation state and reducing the melanin content after UVB rays' exposure [23,24]. In this study, we showed that, similarly to the extract effect, but without the use of solvents or depletion of the microalgal biomass, *TC*-ALG improves human skin cell viability after UVB exposure while exerting potent antioxidant effects. We also found that *TC*-ALG possess anti-melanogenic properties, likely modulating the expression of tyrosinase, a key enzyme in melanin biosynthesis, with a depigmenting effect that is comparable to that of arbutin, a widely used cosmetic ingredient. These findings, along with the advantages of a controllable, efficient, and renewable bioprocess, position nanoalgosomes as a next-generation, sustainable alternative for advanced dermocosmetic treatments against photoaging.

2. Materials and methods

2.1. TC-ALG isolation

TC-ALG isolation was performed from a 6 L culture of the microalga *Tetraselmis chuii* (CCAP 66/21b), grown in F/2 medium, after 30 days of cultivation at a temperature of 20°C ± 2°C with continuous air flow and exposed to white light with a 14 h light and 10 h dark period [25]. The bottles were gently agitated every day to homogenize the cultures and 0.22 μm filters were placed at the bottle inputs to keep microalgae cultures in axenic conditions. Cell growth was evaluated every week using OD600 and cell viability using fluorescein diacetate (Thermo Fisher). Small extracellular vesicle isolation and concentration were performed using the Repligen KrosFlo® KR2i TFF System (Spectrum Labs, Los Angeles, CA, USA) with three different GE Healthcare polysulfone hollow fiber membranes, as described by Adamo et al. (2021) [7,25]. The obtained samples were diafiltrated seven times to make a change buffer in phosphate-buffered saline without calcium and magnesium (PBS).

2.2. TC-ALG characterization

TC-ALG were characterized with biophysical and biochemical methods, following MISEV2018 and 2023 guidelines [4,26], and as reported previously [7].

Nanoparticle tracking analysis (NTA) was performed by NanoSight NS300 (Malvern Panalytical, UK) to assess *TC*-ALG concentration and the size distribution. *TC*-ALG were diluted in HPLC-grade water (Sigma Aldrich), followed by 0.22 μm filtration to ensure the absence of particles (Whatman Anotop filters), to have 20–120 particles per frame. Five 60-second videos were analysed for each sample (n = 3) by NTA software Build 3.1.46, in light scattering, using a detection threshold set to 5 and the camera level at 15–16.

Nanoparticle tracking analysis in fluorescence (F-NTA) was determined using Di-8-ANEPPS-labelled *TC*-ALG (Ex/Em ~465/635 nm, Thermo Fisher Scientific), a dye that emits fluorescence when in presence of EVs lipidic membranes, following Adamo et al. (2021) protocol [7]. In brief, *TC*-ALG were incubated 1 h at room temperature with Di-8-ANEPPS and analysed by NTA equipped with a 500LP filter (480 nm laser).

BCA assay was used to evaluate the protein concentration of *TC*-ALG preparations using micro-bicinchoninic BCA Protein Assay Kit (Thermo Fisher Scientific). This is a colorimetric assay which uses a bovine serum albumin to generate the standard curve. The BCA reaction solution absorbance was measured by GloMax Discover Microplate Reader at 560 nm.

DetectEV assay was used to evaluate the bioactivity and membrane integrity of three different batches of *TC*-ALG. 2×10^{10} nanoalgosomes were incubated with 18 μM fluorescein diacetate (FDA; Sigma-Aldrich) in 0.2 μm-filtered phosphate-buffered saline (PBS) without Ca^{2+} and Mg^{2+}, in a final volume of 200 μL in a 96-well microplate. A negative control consisting of PBS containing the same concentration of FDA (without EVs) was included to assess lack of substrate hydrolysis (background signal). Fluorescence emission was monitored for 180 min at room temperature using the blue filter (excitation: 488 nm) of the GloMax Discover Microplate Reader (Promega). *TC*-ALG enzymatic activity was determined according to the protocol already described and validated previously [9,25,27,28]. A standard calibration curve was established using fluorescein sodium salt (Ex/Em ~490/514 nm; Sigma-Aldrich), diluted in Ca^{2+}- and Mg^{2+}-free PBS to final

concentrations ranging from 300 nM to 0 nM, with a total volume of 200 µL. Data analysis was performed by subtracting the fluorescence intensity of the negative control from the *TC*-ALG samples. Fluorescence values were interpolated onto the standard curve to determine the concentration of generated fluorescein. Finally, the extracellular vesicle-associated enzymatic activity was expressed in enzymatic units (U), defined as the rate of fluorescein production (nM/min), calculated by dividing the concentration of produced fluorescein by the total incubation time [27].

Atomic Force Microscopy (AFM) to assess *TC*-ALG morphology was performed using Nanowizard III scanning probe microscopy (JPK instruments) with a 15 µm z-range scanner. *TC*-ALG were resuspended in MilliQ water to obtain a specific concentration of 5 × 1011 particles/mL and 30 µL aliquot of the sample was deposited for 10 min onto freshly cleaved mica. The surface was then gently dried under a nitrogen stream. Images were acquired using an NSC-15 cantilever (Mikromasch), featuring a typical spring constant of 40 N/m and a tip radius of 8 nm.

Immunoblotting was performed with protein extracts from *TC*-ALG, microalgal cell (*Tetraselmis chuii*), bacteria (*Escherichia coli*) and HEK-293 RIPA-based lysates and separated by sodium dodecyl-sulfate polyacrylamide gel electrophoresis (SDS–PAGE). Prior to electrophoresis, 5 µg of protein from each sample were combined with 5x loading buffer (containing 0.25 M Tris-HCl pH 6.8, 10 % SDS, 50 % glycerol, 0.25 M dithiothreitol, and 0.25 % bromophenol blue). The mixtures were then heated to 100 °C for 5 min and then loaded in two SDS-PAGE. Electrophoretic separation was followed by proteins transfer onto polyvinylidene difluoride (PVDF) membranes. The two different membranes were blocked at room temperature for 1 h in a solution of 3 % bovine serum albumin (BSA) in TBS-T (Tris-buffered saline with 0.05 % Tween-20). Primary antibodies against H^+-ATPase (1:1000, Agrisera), Alix (clone 3A9, 1:150, Santa Cruz), actin plant (clone 10-B3, 1:500, Sigma-Aldrich), OmpA (111228, 1:2000, Antibody Research), and CD81 (clone B-11, 1:100, Santa Cruz) all diluted in blocking solution, were incubated overnight at 4°C and 2 h at room temperature. After washing steps, membranes were incubated for 1 h with species-specific HRP-conjugated secondary antibodies (Cell Signaling). Blots were then washed thoroughly (four washes for 20 min, in TBS-T), and signal detection was carried out using the SuperSignal Pierce ECL (Thermo Fisher Scientific).

2.3. Tetraselmis chuii extract preparation

Tetraselmis chuii cultures were also used to prepare a methanolic extract. Starting from 60 mg of dry biomass, 10 mL of methanol were added, and the sample was subjected to magnetic stirring for 30 min. After agitation, the sample was centrifuged at 3000 × g for 5 min. The resulting supernatant was then carefully removed, and the extraction steps were repeated until a clear methanolic solution was obtained. The collected methanolic fractions were pooled and concentrated using a rotary evaporator (IKA RV 10, Germany) to eliminate the solvent under reduced pressure. After evaporation, the resulting residues were subjected to overnight vacuum drying to ensure complete removal of any residual solvent. A total of 4 mg (dry weight) of the methanolic extract was then resuspended in a water and methanol mixture (2:1, v/v) and an equal volume of diethyl ether was then added. Following vortexing, the mixture was left to enable phase separation. The upper organic phase was collected, and anhydrous sodium sulphate was added to remove residual water. Final solvent removal was carried out using a rotary evaporator until complete evaporation was achieved. After 24 h, the dry extract was dissolved in DMSO (vehicle) at 400 µg/mL (dry dry weight *TC*-extract in DMSO) and stored at –20°C for further analysis.

2.4. Cell culture

For this study, normal human dermal fibroblasts (NHDF) and human melanoma cells (A375) were chosen as cellular models. The NHDF and A375 cell lines were maintained in culture at 37°C with 5 % CO_2 in Dulbecco's Modified Eagle's Medium (DMEM) (Sigma-Aldrich), containing 10 % (v/v) fetal bovine serum (FBS) (Gibco, Life Technologies), with 2 mM L-glutamine, 100 U/mL penicillin, and 100 mg/mL streptomycin (Sigma-Aldrich).

2.5. Viability of human skin cells in vitro following TC-ALG treatment

The NHDF and A375 cells were plated in 96-well plates at a density of 2 × 103 cells/well and maintained in culture for 24 h in their own medium at 37°C with 5 % CO_2. The viability assay was conducted by incubating *TC*-ALG at two different concentrations, 0.5 and 2 µg/mL (corresponding to about 1 ×109 and 4 ×109 *TC*-ALG particles/mL) [7,29]. After 24 h of culture, the treatment was performed with the two concentrations of *TC*-ALG and incubated for 24, 48 and 72 h. A group of cells had their medium replaced with fresh medium and were used as a negative control (100 % viability). Cell viability was evaluated using CellTiter 96 Aqueus One Solution Reagent (Promega) and after 3 h of incubation the absorbance (OD, Absorption at 490 nm) was calculated. The optical density was used to calculate the percentage of live cells using the following formula:

%Percentage of viability = (Treated cells-Blank)/(Control cells-Blank) x 100

The experiment was performed in triplicate and with three different *TC*-ALG' batches and ± SD of the three replicates was calculated.

2.6. In vitro evaluation of irritating potential of TC-ALG in Reconstructed Human Epidermis (OECD 439)

Skin irritation potential of *TC*-ALG was evaluated using SkinEthic™ Reconstructed Human Epidermis (RHE) model, in accordance with the OECD 439 guideline. The study was conducted through an external service with Dermaclaim Lab s.r.l. Briefly, RHE tissues were treated topically with 0.5 µg/mL of *TC*-ALG for 42 min and leaved in culture for 42 h. After the incubation period, tissue viability was assessed using MTT (3-(4,5-Dimethylthiazol-2-yl)-2,5-Diphenyltetrazolium Bromide) cell viability assay, and results were expressed as percentage of viability relative to negative control tissues. Negative (DPBS) and positive controls (5 % SDS) were included.

2.7. Cellular uptake of TC-ALG and endosomal localization study

The cells were plated in 24-well plates containing sterile cover slips at a density of 3 × 104 cells/well and incubated for 24 h at 37°C with 5 % CO_2. After 24 h, *TC*-ALG labelled with Di-8-ANEPPS, following unbound dye removal, were incubated at concentrations of 0.5 and 2 µg/mL; *TC*-ALG -free PBS with the same amount of fluorescent dyes, following dye removal, were incubated and served as negative control (negCTL) [9]. After 3, 6 and 24 h, two washes with PBS were performed, followed by fixation with 3.7 % paraformaldehyde for 15 min and then two more washes with PBS. The nuclei were stained in blue with DAPI (VECTASHIELD Mounting Medium, Promega) [7]. The localization of *TC*-ALG was evaluated using fluorescence microscopy (EVident Olympus). All the images were acquired with the same fluorescence settings (DAPI Ex/Em~345/455, GFP Ex/Em~470/508 with an exposure time of 200 ms for NHDF, and 1 s for A375). The reported relative green fluorescence intensities correspond to the fluorescence intensities of 3 different images of each sample, normalized to the number of nuclei, and relative to the control sample (negCTL). Experiments were repeated using three independent *TC*-ALG preparations.

To evaluate the *TC*-ALG colocalization with the protein CD63, an endosomal marker, first *TC*-ALG were labelled with PKH26 (Ex/Em ~551/567 nm, Sigma Aldrich), as described in Adamo at al. (2021) and Picciotto et al. (2022) [7,30]. Briefly, PHK26 was prepared at a final

concentration of 8 μM in Diluent C (supplied by Sigma-Aldrich with the PKH26 kit). This labelling solution was then incubated with nano-algosome samples at a concentration of 5 × 10 [1] ⁰ particles/mL for 1 h at 37 °C. Cells were grown at a density of 3 × 104 cells/well in 24-well plates containing sterile coverslips in complete medium and, after 24 h, cells were incubated with 2 μg/mL of PKH-26-labeled *TC*-ALG at 37°C for 24 h [7,30]. Cells were fixed with 3.7 % paraformaldehyde for 15 min at room temperature (RT) and washed twice with PBS. Cells were then permeabilized with 1 % Triton X-100 in PBS for 10 min at RT. Afterwards, cells were incubated with blocking solution (1 % bovine serum albumin in PBS) for 30 min at room temperature. Cells were incubated in a primary antibody (anti-CD63, clone MX-49.129.5, Santa Cruz), After three washes with PBS, cells were then incubated with a secondary antibody (AlexaFluor-488; Thermo Fischer Scientific) and diluted in blocking solution (1:50) for 2 h at room temperature. Coverslips were mounted with a drop of Vectashield Mounting Medium with DAPI (Sigma-Aldrich). *TC*-ALG intracellular localization was monitored by fluorescent microscopy (EVident Olympus) [7].

2.8. UVB irradiation

UVB exposure was performed using a UVB lamp (312 nm peak) at 300 J/m^2 for 42 s, setting the exposure to have about 40 % of cell death. The cells (*i.e.*, NHDF and A375 cells) were kept in a small volume of phosphate-buffered saline (PBS) during irradiation [31,32]. After UVB exposure, PBS was replaced with fresh medium, and cells were kept in culture for 24 and/or 48 h.

2.9. Assessment of antioxidant activity of TC-ALG in UVB-irradiated skin cells

Intracellular ROS levels of living cells were determined using 2,7-dichlorofluorescein diacetate (DCFH-DA; Sigma-Aldrich). This non-fluorescent probe emits fluorescence in the presence of ROS in a directly proportional manner, allowing a quantitative assessment of oxidative stress by ROS evaluation. The NHDF and A375 cells were plated in a 96-well plate at a density of 5 × 103 cells/well and incubated at 37°C with 5 % CO_2 in William's E medium without phenol red (Gibco™). After 24 h, both cell lines were treated with two different concentrations of *TC*-ALG (0.5 and 2 μg/mL). As negative control, untreated cells were incubated with fresh medium to set ROS basal level, and as antioxidant-positive control, other cells were treated with 70 μg/mL of arbutin, due to its proven antioxidant effect. After 24 h of treatment, cells were exposed to UVB light, as described before. Next, cells were incubated with DCFH-DA, at a concentration of 40 μM diluted in medium without FBS for 1 h at 37°C with 5 % CO_2. Moreover, cells treated with a 250 μM solution of tert-butyl hydroperoxide (TBH, Sigma-Aldrich) diluted in medium without FBS and incubated for 1 h at 37°C with 5 % CO_2, were used as oxidative-positive control using an oxidizing agent distinct from UVB radiation. After 24 h, both cell lines were treated with two different concentrations of *TC*-ALG (0.5 and 2 μg/mL) and with three different concentrations of *TC*-extract (1, 2, and 5 μg/mL of dry weight of *TC*-extract in DMSO, in NHDF only). After 1 h, intensive washes with PBS with calcium and magnesium were performed and fluorescence was read (Ex/Em ~485/538 nm) using the GloMax Discover Microplate Reader [9,25]. The relative percentage of intracellular ROS was normalized with respect to untreated cells (negative control).

2.10. Photoprotective role of TC-ALG on cell viability after UVB exposure

The NHDF and A375 cells were seeded in 96-well plates at a density of 5 × 103 cells/well and maintained in culture for 24 h in their own medium at 37°C with 5 % CO_2. Two concentrations of *TC*-ALG (0.5 and 2 μg/mL) were used for the experiment, with treatments carried out using three different strategies: 24 h of pre-incubation with *TC*-ALG followed by UVB exposure, *TC*-ALG incubation during the UV exposure and the third *TC*-ALG incubation after UVB exposure. As negative control, untreated cells were incubated with fresh medium (100 % viability); as positive control cells were treated with 70 μg/mL (257 μM) of arbutin (Sigma Aldrich) [33]. After UVB exposure, cells were kept in culture for 24 h for the three conditions, next, the photoprotective role of *TC*-ALG was evaluated using CellTiter 96 Aqueus One Solution Reagent, as described before [24].

2.11. Protective effects of TC-ALG on UVB-induced cell damage in human dermal fibroblasts

Senescence-associated β-galactosidase (SA-β-gal) staining was carried out using a commercially available kit (Sigma-Aldrich CS0030) based on a histochemical stain for β-galactosidase activity at pH 6 using its substrate X-gal (5-bromo-4-chloro-3-indolyl-beta-D-galacto-pyranoside). Following the manufacturer's protocol, cells were seeded in 24 well/plate at a density of 1 × 104 cell/well, and after 24 h cells were treated with/without 0.5 μg/mL of *TC*-ALG; this concentration was chosen following antioxidant and photoprotective results. After 24 h cells were exposed to UVB rays (300 J/m^2) and leaved in culture for 24 h. To perform the SA-β-gal staining, cells were first washed twice in PBS and subsequently fixed with Fixation Buffer for 6 min at room temperature. After fixation, cells were washed three times with PBS, stained with 1 mL of Staining Mixture and incubate for 24 h at 37 °C in a non-CO_2 humidified incubator. Stained cells were then visualized under a light microscope (OLYMPUS, CKX3-SLP), and SA-β-gal-positive cells were quantified acquiring 14 fields/condition (≈800 nuclei/condition) and analysing by ImageJ software (National Institutes of Health, USA). The percentage of SA-β-gal-positive cells (senescent cells) was calculated relative to the total number of cells counted [34,35].

Western Blot analysis of p16 was conducted seeding 1 × 10^4 NHDF cells/well, in 24 well/plate, in their own medium at 37°C with 5 % CO_2 and after 24 h we treated with/without *TC*-ALG at 0.5 μg/mL. After 24 h of treatment we expose cells to UVB rays at 300 J/m2 to induce senesce. After 24 h we detached cells using a scraper and total proteins were extracted by the RIPA buffer and separated by 12 % SDS-PAGE. A total of 10 μg of cell lysate were mixed with 5X loading buffer (0.25 M Tris-Cl pH 6.8, 10 % SDS, 50 % glycerol, 0.25 M dithiothreitol (DTT), 0.25 % bromophenol blue) and heated at 100°C for 5 min. Proteins were electro-transferred onto a polyvinylidene difluoride membrane (PVDF), and the non-specific antibodies were blocked by incubating with 3 % BSA in TBST 1X (50 mM Tris HCl pH 8.0, 150 mM NaCl with 0.05 % Tween-20). Anti-p16 (abcam, AB108349) primary antibody was incubated 1:2000, 1 h at room temperature (RT). Afterwards, anti-rabbit IgG secondary antibody HRP-conjugated was incubated for 1 h at RT. The immunoblot was revealed with SuperSignal Pierce ECL (Thermo Fisher Scientific).and the densitometric analysis was conducted using Image Lab 6.1 BIO-RAD software, in which p16 bands density was normalized to the total protein levels determined by Ponceau S staining.2.12. Anti-melanogenic effect of *TC*-ALG in human melanoma cells

The A375 cell lines were plated in 6-well plates at a density of 1 × 105 cell/well and incubated at 37°C with 5 % CO_2 in complete DMEM reaching 60 % of confluency. Next, cells were pre-treated with 0.5 and 2 μg/mL of *TC*-ALG, and with 70 μg/mL of arbutin. As negative controls, untreated cells were used to set the melanin basal level. After 24 h, cells were exposed to UVB rays or with 200 nM of α-melanocyte stimulating hormone (α-MSH, Sigma Aldrich), to stimulate melanin production. After 48 h, melanin extraction was performed following Ruri Lee et al. [33]. Briefly, cells were detached using a cell scraper, counted using Thoma counting chamber, and 1 million cells per condition were collected and centrifuged at 1000 rpm for 5 min. The resulting pellets were dissolved in 1 N NaOH containing 1 % DMSO. Each sample were then incubated at 80°C with shaking at 250 rpm for 1 h. Cell lysates were transferred to a 96-well plate, and melanin content was measured by reading absorbance at 405 nm using a GloMax Discover Microplate

Reader. A standard curve of melanin (0–100 μg/mL) was prepared using a synthetic melanin (Sigma Aldrich) dissolved in 1 N NaOH [33].

2.12. Anti-tyrosinase activity of TC-ALG in human melanoma cells

Western blot analysis: for tyrosinase expression study, A375 cells seeded and treated using the same experimental setting described in section 2.9. After 24 h, cells were lysed, and total proteins were extracted by the RIPA buffer and separated by 10 % SDS-PAGE. A total of 10 μg of cell lysate were mixed with 5X loading buffer (0.25 M Tris-Cl pH 6.8, 10 % SDS, 50 % glycerol, 0.25 M dithiothreitol (DTT), 0.25 % bromophenol blue) and heated at 100°C for 5 min. Proteins were electro-transferred onto a polyvinylidene difluoride membrane (PVDF), and the non-specific antibodies were blocked by incubating with Odyssey Blocking Buffer (Li-COR) in TBST 1X (50 mM Tris HCl pH 8.0, 150 mM NaCl with 0.05 % Tween-20). Anti-Tyrosinase (TYR) (antibodies.com, [T311] A250239) primary antibody was incubated 1:1000 at 4°C over night and 2 h at room temperature (RT). Afterwards, 1:10000 IRDye® 800CW Goat anti-Mouse IgG secondary antibody (LI-COR) was incubated for 1 h at RT [33]. The immunoblot was revealed with Odyssey LI-COR and the densitometric analysis was conducted using Image Lab 6.1 Bio-Rad software, in which tyrosinase band density was normalized to the total protein levels determined by Ponceau S staining.

For the immunofluorescence study, A375 were seeded in 24-well plate with sterile coverslips, at a density of 3 × 104 cell/well and incubated at 37°C with 5 % CO_2 in complete DMEM. Cells were treated with 0.5 μg/mL of *TC*-ALG and after 24 h of incubation, 200 nM of α-MSH was added for 24 h. Next, cells were fixed with 3.7 % paraformaldehyde for 15 min and then were washed twice with PBS. Cells were permeabilized with 0.1 % Triton X-100 (Sigma Aldrich) in PBS for 5 min at RT and then blocked with 1 % BSA for 30 min at RT. Anti-tyrosinase antibody was added o/n at 4°C diluted 1:1000 in 1 % BSA [36]. Cells were then incubated with a secondary antibody (Alexa-Fluor-488; Thermo Fischer Scientific) and diluted in blocking solution (1:50) for 2 h at room temperature. Coverslips were mounted with a drop of Vectashield Mounting Medium with DAPI (Sigma-Aldrich) and images were taken with Evident Olympus fluorescence microscope. The fluorescence intensity analysis was performed using three different fields/condition, analysing a minimum of 18 nuclei per field, using ImageJ software.

2.13. Statistical analysis

All experiments were repeated independently at least 3 times, with data expressed as mean ± SD. Statistical analysis and graphs were conducted using GraphPad Prism 8 (GraphPad Software Inc., USA). Statistical comparisons were performed using one-way or two-way ANOVA (three or more groups), with Tukey's or Dunnett's multiple comparisons test. Statistical significance was considered at $p < 0.05$. Significance levels were denoted as follows: *$p < 0.05$, **$p < 0.01$, ***$p < 0.001$, and ****$p < 0.0001$. Non-significant differences are indicated as "ns".

3. Results

3.1. Isolation and quality checking of Tetraselmis chuii-derived nanoalgosomes (TC-ALG)

The isolation of *TC*-ALG from the conditioned media of the marine chlorophyte microalgae *Tetraselmis chuii* (*TC*) was carried out using Tangential Flow Filtration (TFF), with sequential 650 nm and 200 nm pore-size cartridges, followed by diafiltration and concentration in phosphate-buffered saline (PBS) using a 500 kDa cut-off membrane [7,9,37]. These preparative steps allowed to concentrate the small EV fraction more than 1000 fold, by obtaining 5 mL samples containing small EVs in PBS from an initial culture volume of 6 L of *Tetraselmis chuii* conditioned media [7,9,26]. The comprehensive characterization of the obtained EV preparation was conducted following MISEV guidelines, allowing us to produce quality-controlled *TC*-ALG preparations in terms of protein and nanoparticle concentration, size distribution, and expression of EV biomarkers (Fig. 1), with high batch-to-batch reproducibility [26].

Across the *TC*-ALG preparations (n = 3), the protein content was 120 ± 20 μg/mL, the particles concentration $5 \times 10^{11} \pm 1 \times 10^{10}$ particles/mL and the size distribution of 110 + /- 10 nm (mode), as measured by Nanoparticles Tracking Analysis (NTA) in scattering mode (Fig. 1a). NTA also indicated that the vesicles displayed a narrow size distribution, consistent with the population of small EVs. Fluorescence NTA analysis was performed using Di-8-ANEPPS-labeled *TC*-ALG, confirmed the presence of membrane-bound particles within the same size range, validating their identity as EVs (Fig. 1b). Furthermore, the ratio between EV particle number and total protein content was consistent across all *TC*-ALG batches (n = 3), with 1 μg of EV protein corresponding to 5–10 × 10^9 particles. This falls within the optimal range for small EVs, as proposed by Sverdlov [38], and allowed to determined that the *TC*-ALG yield is 50–100 μg of EV protein per Liter of TC-conditioned media, corresponding to $1 \times 10^{12} \pm 5 \times 10^{10}$ *TC*-ALG/L of *TC*-conditioned media. These results were further validated through atomic force microscopy (AFM), which confirmed the *TC*-ALG morphology as typical of small EVs (Fig. 1c). Furthermore, protein profiling through SDS-PAGE and immunoblotting detected canonical EV markers such as H^+-ATPase and Alix as well as Actin in *TC*-ALG. These molecular signatures support the successful isolation of highly enriched EV preparations (Fig. 1d). Collectively, these results confirm that the nanoalgosomes derived from *Tetraselmis chuii* possess characteristic nanoscale dimensions, structural integrity, and marker protein expression typical of small EVs. Moreover, to ensure the functional quality of the specific *TC*-ALG batches used in this study, we performed the DetectEV enzymatic assay [9,28]. This assay measures the conversion of non-fluorescent fluorescein diacetate (FDA) into fluorescein by active intraluminal esterases, a reaction that relies on vesicle membrane integrity. The assay included a negative control consisting of PBS incubated with the same amount of FDA, which was used to measure the non-specific background hydrolysis. This background value was subtracted from the fluorescence intensity of the *TC*-ALG samples. As shown in Supplementary Figure 1, we observed a specific, time-dependent increase in fluorescence in the *TC*-ALG samples (n = 3). The quantification of this activity yielded a rate of 1.5 ± 0.3 nM/min. Notably, this value is fully consistent with the bioactivity range previously reported for high-quality nanoalgosome preparations, confirming the reproducibility of the production process and the suitability of the batches employed for the subsequent skin cell experiments [27,28]. [27].

3.2. TC-ALG biocompatibility and internalization in human skin cells

The biocompatibility of *TC*-ALG was evaluated in normal human dermal fibroblasts (NHDF) and human melanoma cells (A375) using the MTS (3-(4,5-dimethylthiazol-2-yl)-5-(3-carboxymethoxyphenyl)-2-(4-sulfophenyl)-2H-tetrazolium) assay (Fig. 1e and f). Moreover, the use of Reconstructed Human Epidermis (RHE) allows us to confirm *TC*-ALG biocompatibility, in a more appropriate 3D skin model. As shown in Fig. 1g, the topical administration of the positive control (SDS 5 %) reduced tissue viability of about 99 %, while *TC*-ALG at 0.5 μg/mL (corresponding to 5 × 10^9 particles/mL) did not have any detrimental effect if compared to the negative control. This results deeper demonstrate the biocompatibility of *TC*-ALG in human skin cells and tissue, and particularly their non-irritant nature.

Once confirmed the non-cytotoxic nature of *TC*-ALG in these skin cells, we performed an uptake study using a green-fluorescent version of *TC*-ALG labelled with the lipophilic dye Di-8-ANEPPS, analysed by fluorescent microscopy. In control cells treated with PBS containing the

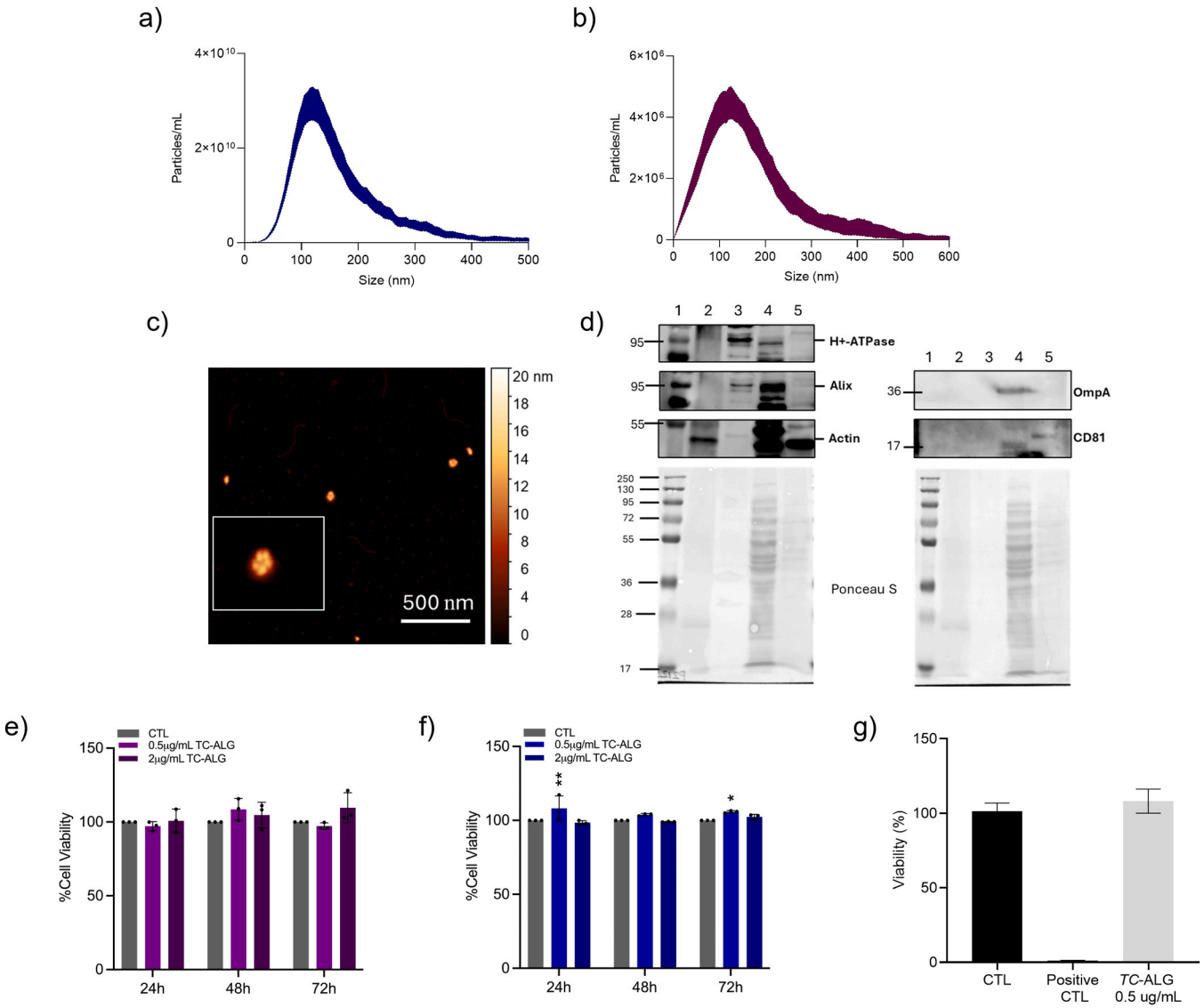

Fig. 1. *TC*-ALG quality check and biocompatibility in skin cells. a) *TC*-ALG concentration and size distribution measured with NTA (blue deviation is relative to five measurements per sample); b) size distribution of Di-8-ANEPPS-labelled *TC*-ALG measured with Fluorescent (F)-NTA (purple deviation is relative to five measurements per sample); c) morphological evaluation of *TC*-ALG using AFM; d) *TC*-ALG positive (e.g., H+-ATPase, Alix and Actin) and negative (e.g. OmpA and CD81) marker expression analysed with immunoblot in 1) marker; 2) TC lysate; 3) TC-ALG; 4) bacteria lysate; 5) HEK lysate. *TC*-ALG biocompatibility evaluation in NHDF (e) and A375 (f) cell, by MTS assay;g) TC-ALG irritating potential in Reconstructed Human Epidermis (RHE), following OECD439 guidelines. Statistical analyses were performed using two-way ANOVA (comparing control vs. treatments at each time point). Differences are reported as not significant (ns) or as *$p < 0.05$, **$p < 0.01$, where indicated. All the images are representative results of three independent replicates.

same amount of fluorescent dyes after dye removal (negCTL), only minimal background fluorescence was detected. In contrast, cells exposed to *TC*-ALG displayed progressively stronger intracellular green fluorescence over time, with a more pronounced signal observed at the higher concentration (2 µg/mL). Quantitative analysis of fluorescence intensity confirmed these observations, showing a significant increase in intracellular fluorescence at both 6 h and 24 h compared to baseline (Fig. 2b). The fluorescence intensity was significantly higher at 2 µg/mL than at 0.5 µg/mL in both cell types (****$p < 0.0001$), indicating that *TC*-ALG internalization is both dose- and time-dependent.

Furthermore, we have observed the intracellular localization (Fig. 2**c**) of PKH26-labelled *TC*-ALG (in red) within the CD63-positive endosomal compartment, through immunostaining for the CD63 protein (in green) in line with previous findings by Adamo et al. (2021) [7, 9].

3.3. *TC-ALG contrasts the UVB-induced damage in skin cells*

Antioxidant activity of TC-ALG: Several studies have explored the antioxidant potential of microalgal extracts in various biological systems [39]. Moreover, such microalgal extracts are already used in commercial cosmetic formulations; however, this raises sustainability challenges linked to the extraction and production processes required to obtain them.

As a preliminary step, we evaluated the antioxidant activity of methanolic extracts of our *Tetraselmis chuii* (*TC*-extract) to verify and confirm consistency with effects reported in the literature [40]. The *TC*-extract was tested at concentrations of 1, 2, and 5 µg/mL of dry weight in DMSO on NHDF cells; oxygen reactive species (ROS) levels were measured following oxidative stimulation with tert-butyl hydroperoxide (TBH). Consistently, the *TC*-extract exerted a significant antioxidant effect, reducing ROS production and better preserving cellular redox balance (Supp. Fig. 2). Having established the extract's

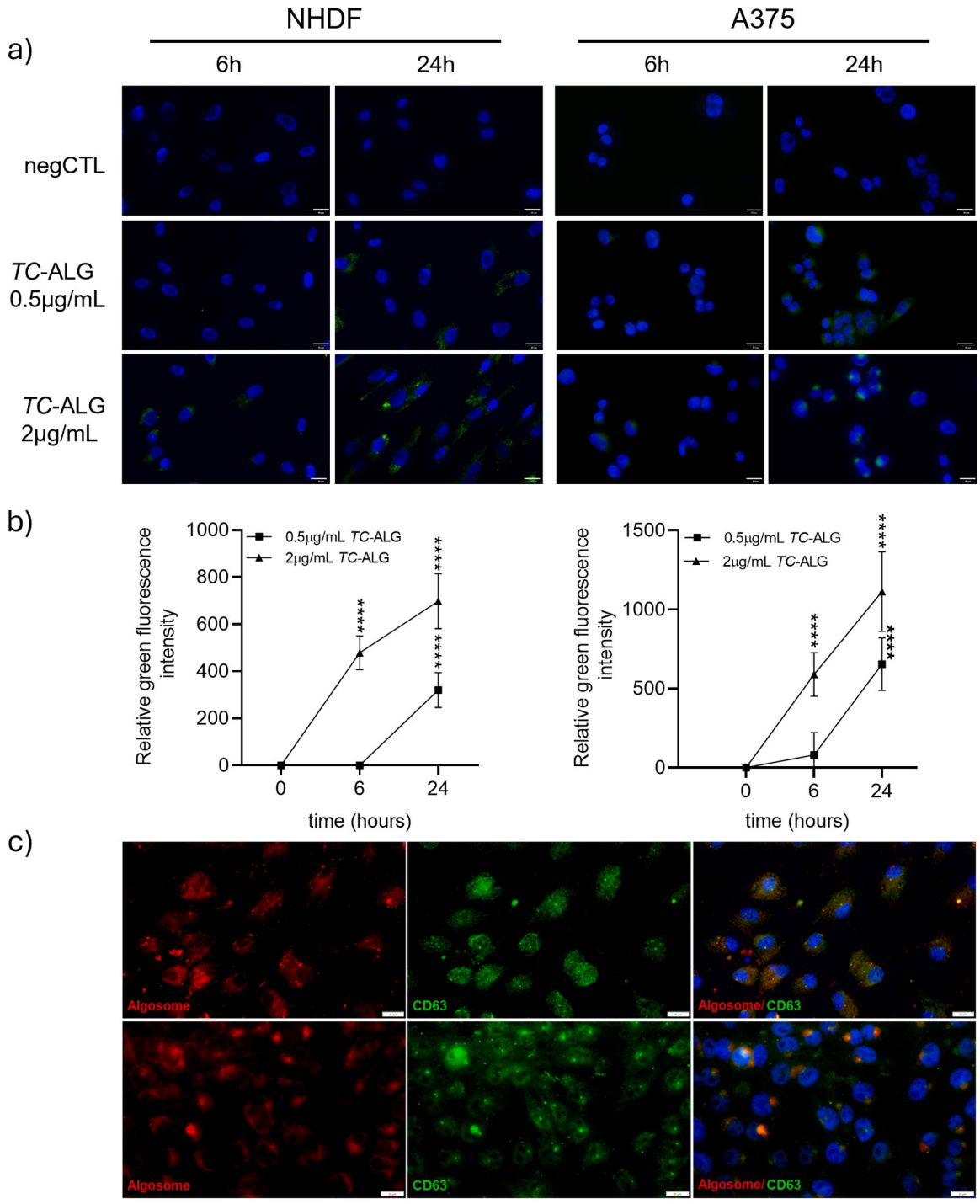

Fig. 2. Cellular uptake and colocalization of CD63 and *TC*-ALG in human skin cells. a) Representative fluorescence microscopy images of NHDF and A375 cell lines, incubated with different concentrations of green labelled TC-ALG for 6 and 24 h, at 37°C. Cells treated with vehicle (PBS) containing the same amount of fluorescent dyes, following dye removal (negCTL), served as negative controls. Nuclei were stained with DAPI (blue), and TC-ALG fluorescence is shown in green. Scale bars, 20 µm. b) Quantification of intracellular fluorescence intensity in NHDF (left) and A375 (right) cells after incubation with TC-ALG at 0.5 µg/mL or 2 µg/mL for the indicated time points. Data are expressed as relative green fluorescence intensity (mean ± SD, n = 3). A significant increase in fluorescence was observed over time and with higher TC-ALG concentrations (****$p < 0.0001$). The statistical analysis was conducted by two-way ANOVA using Dunnett's multiple comparison test (negative control vs. TC-ALG) for each concentration and time; ****$p < 0.0001$. c) Representative immunofluorescence microscopy images that show intracellular uptake of PKH26 fluorescent TC-ALG (in red) in NHDF (upper panel) and A375 (lower panel) cell lines (nuclei in blue) and the co-localization with the endosomal marker CD63 (in green). Magnification 40X, scale bar 20 µm. All the images are representative results of three independent replicates.

antioxidant potential as a control, we then focused our experiments on *TC*-ALG, which offer a solvent-free, cost-effective, and reproducible alternative to conventional microalgal extracts.

UVB rays are the ones responsible of DNA damage, solar erythema, photodamage, melanin synthesis and ROS production in cutaneous cells [41,42]. Previous studies demonstrated *TC*-ALG' antioxidant activity *in vitro* (*e.g.* in breast cancer and non-tumorigenic mammary epithelial cell lines) and *in vivo* using H_2O_2 and TBH as oxidant agents, confirming also

the absence of oxidant effect of *TC*-ALG per se [9]. In this study, the antioxidant role of nanoalgosomes was further investigated using UVB rays to induce ROS production in human skin cells. For this experiment, NHDF and A375 cells were pre-treated for 24 h with two different concentrations of *TC*-ALG before UVB exposure. In parallel, cells were treated for 24 h with arbutin, a natural compound with well-established anti-melanogenic activity and reported antioxidant properties, used here as a positive control in UVB-related effects studies [43,44]. First, we confirm that arbutin treatment did not have any toxic effect in both cell lines used, performing an MTS assay and evaluating cell viability (Supp. Fig. 3a and b). Following the 24 h of pre-incubation, cells were exposed to UVB radiation; UVB treatment significantly increased ROS production in both skin cell lines, similar to what observed upon the TBH-stimulation, confirming that UVB exposure severely affects cellular health by elevating intracellular ROS levels (Fig. 3a and b). Notably, 24 h pretreatment with *TC*-ALG effectively reduces ROS levels in UVB-exposed cells, restoring their oxidative status to basal levels. Remarkably, nanoalgosomes exhibit an antioxidant effect comparable to that of arbutin (Fig. 3a and b). This finding suggests that nanoalgosomes may serve as a potential alternative to conventional antioxidant compounds in preventing oxidative stress.

Photoprotective activity of TC-ALG: Given the previously observed antioxidant activity of *TC*-ALG in human skin cells, their potential to mitigate or prevent UVB-induced cellular damage was investigated by assessing cell viability in NHDF and A375 cell lines. Both cell lines were exposed to UVB radiation (300 J/m^2) and subjected to three different

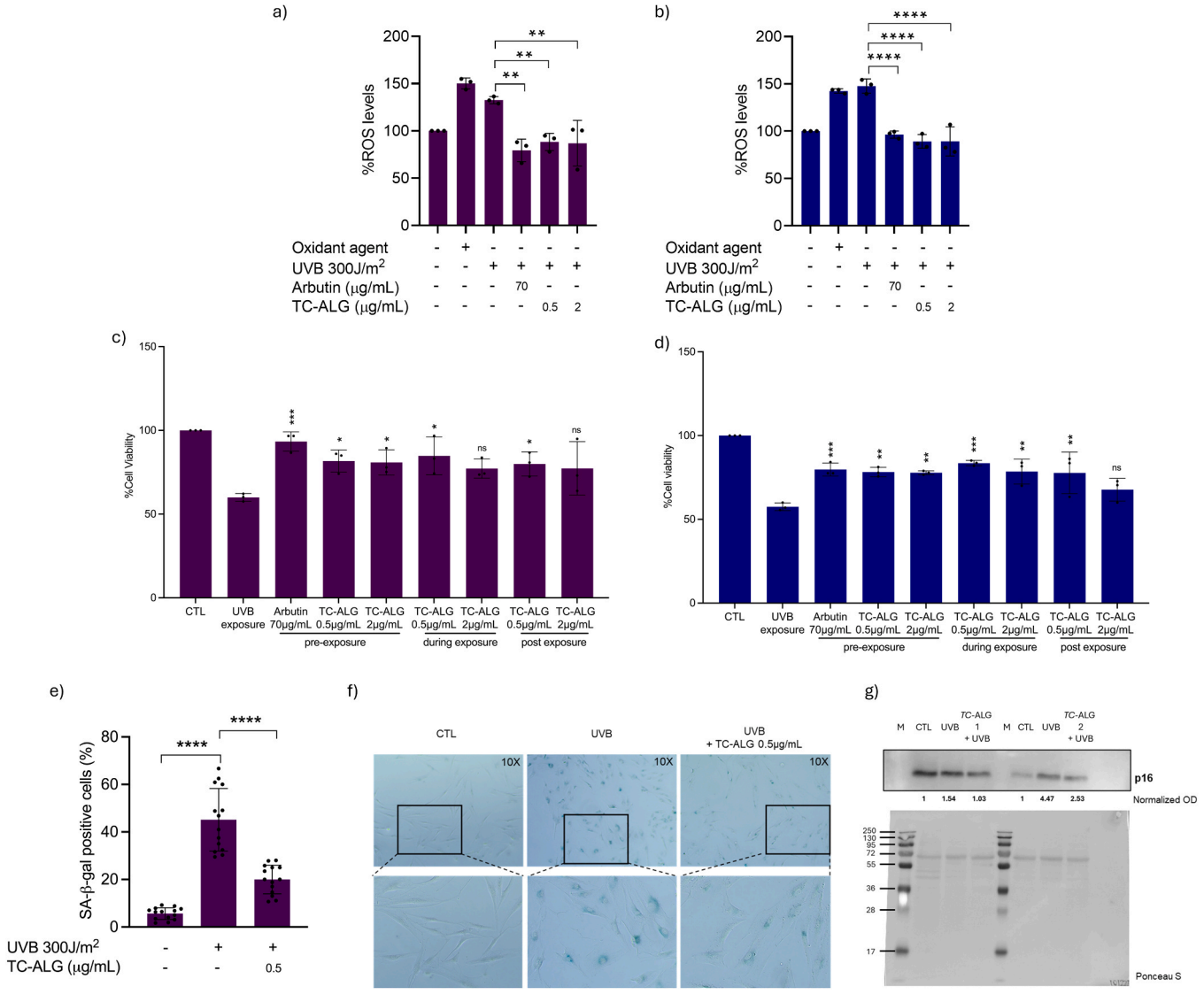

Fig. 3. Antioxidant, photoprotective and anti-photoaging role of *TC*-ALG after UVB exposure in human skin cells. Panels (a) and (b) show the percentage of intracellular ROS level in NHDF and A375 cells, respectively, following treatment with *TC*-ALG (0.5 and 2 µg/mL), either alone or in combination with an oxidative stressor (250 µM TBH) or UVB exposure (300 J/m2). In both cell lines, *TC*-ALG markedly reduced ROS accumulation, highlighting its antioxidant potential. Panels (c) and (d) illustrate the positive effect of *TC*-ALG (0.5 and 2 µg/mL) on cell viability before, during and after 24 h of UVB irradiation in NHDF and A375 cells, respectively, indicating a clear photoprotective role. Panel (e) depicts the anti-photoaging activity of *TC*-ALG, expressed as the percentage of SA-β-gal-positive cells following UVB exposure, with or without *TC*-ALG treatment. Panel (f) presents representative bright-field images of SA-β-gal staining, visually confirming the reduction in senescence markers in *TC*-ALG-treated samples. The statistical analysis (UVB exposure *vs.* treatments) was conducted by ordinary one-way ANOVA *p < 0.05, **p < 0.01, ***p < 0.001, ****p > 0.0001. In e) data are presented as individual values, with each dot corresponding to the percentage of SA-β-gal positive cells per field (n = 14 fields per condition). Images are representative results of three independent replicates. Panel (g) represent the immunoblot blot analysis of p16 in NHDF cells after UVB exposure and with two different *TC*-ALG preparations (batch 1 and 2) treatment at 0.5 µg/mL. Optical density (OD) of each band was normalized to the corresponding Ponceau S staining. The OD was then compared with the control (CTL, untreated cells) to determine fold changes, which are reported as normalized OD values.

TC-ALG treatment approaches to evaluate their potential effects against UVB-induced damages. Arbutin was included as a positive control [45]. Fig. 3c and d show how UVB rays' exposure resulted in a 45 % reduction in viability for both skin cell lines compared to the not exposed control (CTL). Instead, treatments with *TC*-ALG, performed 24 h before, during, or after UVB exposure, succeeded in significantly restoring viability levels. This result demonstrates the photoprotective role of *TC*-ALG, with an effect comparable to arbutin, even at a very low concentration (0.5 μg/mL, corresponding to 5×10^9 particles/mL). The ability of *TC*-ALG to improve cell viability is likely linked to its capacity to modulate ROS production and mitigate their harmful effects. Notably, *TC*-ALG contrasts the UVB-induced cell damage when administered as a pre-treatment (before UVB exposure, preventing damage), as a co-treatment (during UVB exposure, contrasting ongoing damage), and as a post-treatment (after UVB exposure, restoring cell balance).

Protective effects of TC-ALG on UVB-induced cell damage: To investigate the potential of *TC*-ALG in protecting cell against UVB-related senescence (UVB-induced photoaging) we evaluated SA-β-galactosidase (SA-β-gal) activity in NHDF following UVB exposure (Fig. 3e and f). This assay exploits the elevated lysosomal β-galactosidase activity that characteristically accumulates in senescent cells and becomes detectable at pH 6.0. Cells were fixed and subsequently incubated with a chromogenic substrate, X-gal, which, upon enzymatic cleavage by SA-β-gal, produces an insoluble blue precipitate. The presence of blue-stained cells was then evaluated microscopically, and the percentage of SA-β-gal positive cells was quantified as relative to the total cell number. As expected, UVB rays considerably increased the number of SA-β-gal-positive cells, indicating enhanced early cellular senescence, while the treatment with 0.5 μg/mL *TC*-ALG significantly reduced SA-β-gal-positive cells compared to the UVB-only group, suggesting an anti-aging

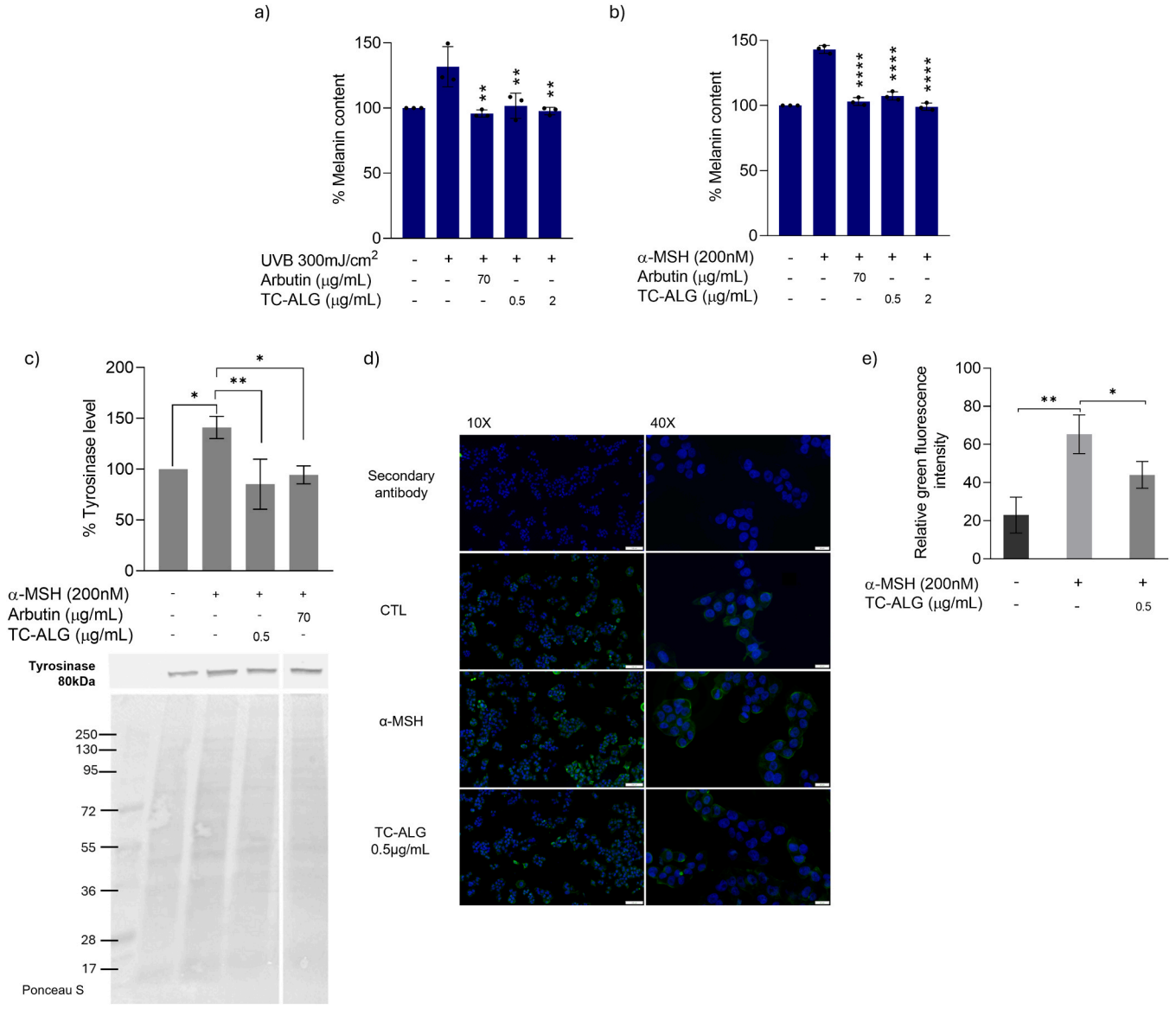

Fig. 4. Anti-melanogenic effect of *TC*-ALG and tyrosinase expression in human melanoma cells after melanin stimulation through UVB or α-MSH. The graph shows the percentage of melanin content extracted from A375 cells after UVB exposure (a) or stimulated with α-MSH (b), demonstrating the anti-melanogenic effect of *TC*-ALG. (c) Representative Western blot of tyrosinase expression (TYR) after α-MSH stimulation and treatment with *TC*-ALG or arbutin. Ponceau S staining was used as loading control. The bar graph shows densitometric quantification of TYR normalized to Ponceau S band intensities. Data are presented as mean ± SD (n = 3). (d–e) Representative immunofluorescence image of tyrosinase (green) (d) and corresponding quantification of relative fluorescence intensity (e). α-MSH stimulation increases tyrosinase fluorescence, while *TC*-ALG pre-treatment reduces it, indicating downregulation of tyrosinase expression. The statistical analyses were conducted by Ordinary one-way ANOVA *p < 0.05, **p < 0.01, ***p < 0.001, ****p < 0.0001, performing Dunnett's multiple comparisons test (UVB exposure or α-MSH *vs.* *TC*-ALG or arbutin). Images are representative results of three independent replicates.

effect of these microalgae-derived EVs.

To confirm the anti-photoaging activity of *TC*-ALG following UVB exposure immunoblot analysis was performed to evaluate the expression of the senescence-associated marker p16 in NHDF cells following UVB irradiation (Fig. 3g). As expected, exposure to UVB radiation (300 J/m^2) resulted in a significant induction of cellular senescence, as evidenced by a marked increase in p16 protein levels, while pre-treatment with *TC*-ALG (0.5 μg/mL) significantly counteracted the UVB-induced upregulation of p16, reducing the protein expression by 38 % ± 10 %. Overall, these results indicate that *TC*-ALG treatment effectively mitigates UVB-induced senescence in NHDF cells, as demonstrated by the down-regulation of key senescence-associated marker.

3.4. Anti-melanogenic and anti-tyrosinase effects of TC-ALG in human melanoma cells

To assess the anti-melanogenic role of *TC*-ALG, we treated human melanoma cells (A375) with two concentrations of *TC*-ALG and exposed them to UVB rays or alpha-melanocyte stimulating hormone (α-MSH) (Supp. Fig. 3c), a peptide released by the pituitary gland that bounds the melanocortin 1 receptor (MC1R), to stimulate melanin production. After 48 h of combined treatment, we extracted melanin using the described protocol, measuring absorbance values at 405 nm and analysing the amount of extracted melanin using synthetic melanin standard curve (Supp. Fig. 4). UVB treatment resulted in a 31 % increase in melanin content, while treatment with arbutin (70 μg/mL) or *TC*-ALG (0.5 and 2 μg/mL) reduced melanin content respectively by 26.7 %, 23.6 % and 25.9 % (Fig. 4a). α-MSH treatment induced an increase of melanin content of 42 %, while arbutin and *TC*-ALG showed an anti-melanogenic effect of respectively of 29.6 %, 25.35 % and 30.9 % (Fig. 4b). These results demonstrate the ability of *TC*-ALG to significantly reduce melanin content, and it is important to highlight that this effect is perfectly comparable to the arbutin, a depigmenting agent already used in cosmetic products that also have a moderate effect on modulating tyrosinase expression and a strong ability in inhibit tyrosinase activity.

To further investigate the specific mechanism by which *TC*-ALG exert their anti-melanogenic activity, tyrosinase (TYR) expression levels were analysed in A375 cells pre-treated with 0.5 μg/mL of nanoalgosomes (the lowest concentration at which significant effects on melanin reduction were observed) or 70 μg/mL of arbutin, followed by stimulation with α-MSH. Densitometric analysis of immunoblot results revealed that the treatment with α-MSH led to an increase in tyrosinase expression levels (Fig. 4c). However, pre-treatment with *TC*-ALG effectively counteracted this effect, restoring tyrosinase expression to basal levels and resulting in an approximate 30 % reduction in protein levels (Fig. 4c). These results were also validated by immunofluorescence (Fig. 4d and e). The representative images show that α-MSH stimulation results in an increased green fluorescence intensity, while *TC*-ALG pre-treatment can reduce this fluorescence and so tyrosinase levels of about 33 %. These results provide further evidence that *TC*-ALG modulates melanogenesis acting on tyrosinase expression and reinforces their potential as depigmenting agents.

4. Discussion

Microalgae are known to produce a wide range of bioactive compounds with different biological activity, most of them related to pigments [46,47]. In our previous investigations, *Tetraselmis chuii* showed the presence of neoxanthin, violaxanthin, lutein, β-carotene and chlorophyll [8]. All these pigments, known for their antioxidant and photoprotective activity, are already used in cosmetic formulations, and some of them showed the ability to reverse aging and melanogenesis mechanisms [47–50]. Moreover, *Tetraselmis chuii* and other microalgal chemical extracts, as well as liposome-based skin delivery technology of natural active ingredients of microalgae, are widely studied and actually used in cosmetics [51–53]. It has been observed, indeed, that the encapsulation of entire microalgae extracts, as well as their single pigments (*e.g.* fucoxanthin or astaxanthin), within liposomes, enhances their thermal stability, absorption, and activity in various cell lines and *in vivo* [51,54]. Our previous studies confirmed that nanoalgosomes possess innate antioxidant and anti-inflammatory activities, due to their endogenous cargo, *in vitro* and *in vivo* [9,10]. Here we demonstrate that these microalgae-derived EVs have a significative activity on contrasting UVB-induced damage in skin cells, acting on the reduction of oxygen reactive species content, and consequently increasing cell viability and reverting photoaging mechanisms.

Moreover, recently main focus of cosmetic and dermatological research turned to the formulation of depigmenting products to treat skin with dark spots caused by UV exposure or pathological conditions like melasma. Unfortunately, most depigmenting agents have shown limitations in term of human safety and ecological footprint: hydroquinone was banned in 2001 due to cytotoxic effect of its metabolites, kojic acid was banned in Japan because of the reported allergic reactions, and the use of arbutin is restricted starting from 2023 [55–58]. The anti-melanogenic effect, which is the ability to reduce the melanin content produced by melanocytes, can be attributed to various mechanisms (e.g., degradation of the pigment, inhibition of the melanogenesis-stimulating hormone, inhibition of tyrosinase expression or activity) [59]. Such anti-melanogenic activities have been tackled over the years by treating melanocytes with various microalgae extracts. For example, it has been demonstrated that the microalga *Pavlova lutheri* can reduce melanin content in B16F10 tumour cells, and that the extract of the cyanobacterium *Phormidium persicinum* displayed an anti-melanogenic properties in human volunteers [60,61]. Given these findings, and considering the pigment profile of *Tetraselmis chuii*, we aimed to evaluate the potential anti-melanogenic effect of nanoalgosomes by measuring melanin content in human melanoma cells stimulated with UVB radiation or α-melanocyte-stimulating hormone. Results showed that nanoalgosomes can significantly reduce the melanin content, confirming a depigmenting activity of these small-EVs. Importantly, the anti-melanogenic effect and the photoprotective role of *Tetraselmis chuii*-derived nanoalgosomes, exerted already at a very low concentration, are perfectly comparable to the effect of arbutin, a well-known anti-melanogenic, antioxidant and photoprotective compound. These results suggest that, similarly to microalgae extracts, microalgae-derived EVs possess diversified beneficial properties and may offer a natural and sustainable alternative to synthetic compounds currently used for skin health treatments. With respect to whole extracts, the use of the microalgal-derived EVs offer several advantages: their biogenesis is a physiological and reproducible process, ensuring strong batch-to-batch consistency; nanoalgosomes' production is solvent-free, rapid, sustainable and renewable, aligning with dermocosmetic market demands for eco-compatible and cost-effective ingredients. Furthermore, extracellular vesicles are naturally evolved to mediate intercellular communication by delivering bioactive molecules, which makes them able of inducing cellular responses and exerting specific biological effects. Unlike extracts, EVs can enrich and protect natural active compounds from microalgae, facilitate their delivery, and enhance their bioavailability, thus boosting efficacy. A limitation of this study is that the photoprotective and anti-melanogenic effects of nanoalgosomes were assessed exclusively *in vitro*, using human skin cell lines. While this is a widely accepted and informative first step to evaluate efficacy, it does not fully represent the structural and functional complexity of human skin. To strengthen the translational relevance of our findings, future studies should include advanced models such as organ-on-chip platforms or *in vivo* human studies, which would help to define nanoalgosomes activity in physiologic conditions.

Overall, our findings highlight the potential of nanoalgosomes (*i.e.*, *TC*-ALG and other microalgae-derived EVs) as multifunctional dermocosmetic ingredients. Specifically, we propose their use both to counteract UVB-induced cellular damage by rebalancing ROS levels, and to reduce melanin synthesis as depigmenting agents for treating existing

UVB-induced hyperpigmentation, such as melasma. These properties make them promising candidates for the treatment of a range of cutaneous alteration.

CRediT authorship contribution statement

Natasa Zarovni: Writing – review & editing. **Antonella Bongiovanni:** Writing – review & editing, Supervision, Methodology, Conceptualization, Funding acquisition. **Giorgia Adamo:** Writing – review & editing, Supervision, Investigation. **Paola Gargano:** Writing – original draft, Methodology, Investigation, Formal analysis, Conceptualization. **Samuele Raccosta:** Writing – review & editing, Investigation. **Estella Rao:** Writing – review & editing, Investigation. **Sabrina Picciotto:** Writing – review & editing, Methodology, Investigation, Formal analysis, Conceptualization. **Angela Paterna:** Writing – review & editing, Investigation. **Mauro Manno:** Writing – review & editing, Investigation, Funding acquisition. **Monica Salamone:** Writing – review & editing, Investigation. **Daniele Paolo Romancino:** Writing – review & editing, Investigation. **Giulia Smeraldi:** Writing – review & editing, Investigation.

Declaration of Generative AI and AI-assisted technologies in the writing process

During the preparation of this work the author(s) used ChatGPT in order to improve language and readability. After using this tool, the author(s) reviewed and edited the content as needed and take(s) full responsibility for the content of the publication.

Funding

This work was supported by the VES4US and the BOW projects, funded by the European Union's Horizon 2020 research and innovation programme, under grant agreements nos. 801338 and 952183; MUR PNRR 'National Centre for Gene Therapy and Drugs based on RNA Technology' (Project no. CN00000041 CN3 RNA); Protein Loaded extracellular vesicles As Next generation Therapeutics (PLANT, Project code 2022TF4BKK), funded by the European Union - NextGenerationEU under the National Recovery and Resilience Plan (NRRP), concession Decree No. 104 of February 2, 2022 adopted by the Italian Ministry of University and Research, Mission 4, Component 2, Investiment 1.1; Programma Nazionale di Ricerca e Progetti di Interesse Nazionale (PRIN); European Brain ReseArch INfrastructureS-Italy (EBRAINS-Italy, Project code IR0000011), funded by the European Union - NextGenerationEU under the National Recovery and Resilience Plan (NRRP), concession Degree No. 117 of June 21, 2022 adopted by the Italian Ministry of University and Research, Mission 4, Component 2, Investment 3.1.

Declaration of Competing Interest

The authors declare the following financial interests/personal relationships which may be considered as potential competing interests: Antonella Bongiovanni reports financial support was provided by National Research Council of Italy. Antonella Bongiovanni reports a relationship with EVEBiofactory srl that includes: board membership. Mauro Manno reports a relationship with EVEBiofactory srl that includes: board membership. Paola Gargano reports a relationship with EVEBiofactory srl that includes: employment. Antonella Bongiovanni has patent #PCT/EP2020/086622 licensed to assignee. Mauro Manno has patent #PCT/EP2020/086622 licensed to assignee. If there are other authors, they declare that they have no known competing financial interests or personal relationships that could have appeared to influence the work reported in this paper.

Acknowledgements

The authors acknowledge Nicolas Touzet and Helen Herbert (ATU, Ireland) and María D. Mayán Santos (CINBIO – University of Vigo, Spain) for support and precious advice, Luca Caruana (CNR-IRIB, Italy) for administrative support and Dermaclaim Lab s.r.l for *in vitro* analysis

Appendix A. Supporting information

Supplementary data associated with this article can be found in the online version at doi:10.1016/j.biopha.2025.118961.

Data availability

I've shared the link to my data (Figshare repository)
research data_gargano (figshare)

References

[1] M. Manno, A. Bongiovanni, L. Margolis, P. Bergese, P. Arosio, The physico-chemical landscape of extracellular vesicles, Nat. Rev. Bioeng. 3 (2024) 68–82, https://doi.org/10.1038/s44222-024-00255-5.

[2] M. Yáñez-Mó, P.R.-M. Siljander, Z. Andreu, A. Bedina Zavec, F.E. Borràs, E.I. Buzas, K. Buzas, E. Casal, F. Cappello, J. Carvalho, E. Colás, A. Cordeiro-da Silva, S. Fais, J. M. Falcon-Perez, I.M. Ghobrial, B. Giebel, M. Gimona, M. Graner, I. Gursel, M. Gursel, N.H.H. Heegaard, A. Hendrix, P. Kierulf, K. Kokubun, M. Kosanovic, V. Kralj-Iglic, E.-M. Krämer-Albers, S. Laitinen, C. Lässer, T. Lener, E. Ligeti, A. Linē, G. Lipps, A. Llorente, J. Lötvall, M. Manček-Keber, A. Marcilla, M. Mittelbrunn, I. Nazarenko, E.N.M. Nolte-'t Hoen, T.A. Nyman, L. O'Driscoll, M. Olivan, C. Oliveira, É. Pállinger, H.A. del Portillo, J. Reventós, M. Rigau, E. Rohde, M. Sammar, F. Sánchez-Madrid, N. Santarém, K. Schallmoser, M. Stampe Ostenfeld, W. Stoorvogel, R. Stukelj, S.G. Van der Grein, M. Helena Vasconcelos, M. H.M. Wauben, O. De Wever, Biological properties of extracellular vesicles and their physiological functions, J. Extracell. Vesicles 4 (2015) 27066, https://doi.org/10.3402/jev.v4.27066.

[3] A.F. Hill, Therapeutically harnessing extracellular vesicles, Nat. Rev. Drug Discov. 21 (2022) 379–399, https://doi.org/10.1038/s41573-022-00410-w.

[4] J.A. Welsh, D.C.I. Goberdhan, L. O'Driscoll, E.I. Buzas, C. Blenkiron, B. Bussolati, H. Cai, D. Di Vizio, T.A.P. Driedonks, U. Erdbrügger, J.M. Falcon-Perez, Q. Fu, A. F. Hill, M. Lenassi, S.K. Lim, M.G. Mahoney, S. Mohanty, A. Möller, R. Nieuwland, T. Ochiya, S. Sahoo, A.C. Torrecilhas, L. Zheng, A. Zijlstra, S. Abuelreich, R. Bagabas, P. Bergese, E.M. Bridges, M. Brucale, D. Burger, R.P. Carney, E. Cocucci, R. Crescitelli, E. Hanser, A.L. Harris, N.J. Haughey, A. Hendrix, A. R. Ivanov, T. Jovanovic-Talisman, N.A. Kruh-Garcia, V. Ku'ulei-Lyn Faustino, D. Kyburz, C. Lässer, K.M. Lennon, J. Lötvall, A.L. Maddox, E.S. Martens-Uzunova, R.R. Mizenko, L.A. Newman, A. Ridolfi, E. Rohde, T. Rojalin, A. Rowland, A. Saftics, U.S. Sandau, J.A. Saugstad, F. Shekari, S. Swift, D. Ter-Ovanesyan, J. P. Tosar, Z. Useckaite, F. Valle, Z. Varga, E. Van Der Pol, M.J.C. Van Herwijnen, M. H.M. Wauben, A.M. Wehman, S. Williams, A. Zendrini, A.J. Zimmerman, M.I.S.E. V. Consortium, C. Théry, K.W. Witwer, Minimal information for studies of extracellular vesicles (MISEV2023): From basic to advanced approaches, J. Extracell. Vesicle 13 (2024) e12404, https://doi.org/10.1002/jev2.12404.

[5] M.A. Kumar, S.K. Baba, H.Q. Sadida, S. Al, J. Marzooqi, F.H. Jerobin, N. Altemani, M.A. Algehainy, A.-B. Alanazi, R. Abou-Samra, A.S. Kumar, M.A. Al-Shabeeb Akil, R. Macha, A.A. Mir, Bhat, Extracellular vesicles as tools and targets in therapy for diseases, Sig. Transduct. Target Ther. 9 (2024) 27, https://doi.org/10.1038/s41392-024-01735-1.

[6] K.W. Witwer, J. Wolfram, Extracellular vesicles versus synthetic nanoparticles for drug delivery, Nat. Rev. Mater. 6 (2021) 103–106, https://doi.org/10.1038/s41578-020-00277-6.

[7] G. Adamo, D. Fierli, D.P. Romancino, S. Picciotto, M.E. Barone, A. Aranyos, D. Božič, S. Morsbach, S. Raccosta, C. Stanly, C. Paganini, M. Gai, A. Cusimano, V. Martorana, R. Noto, R. Carrotta, F. Librizzi, L. Randazzo, R. Parkes, U. Capasso Palmiero, E. Rao, A. Paterna, P. Santonicola, A. Iglič, L. Corcuera, A. Kisslinger, E. D. Schiavi, G.L. Liguori, K. Landfester, V. Kralj-Iglič, P. Arosio, G. Pocsfalvi, N. Touzet, M. Manno, A. Bongiovanni, Nanoalgosomes: Introducing extracellular vesicles produced by microalgae, J. Extracell. Vesicle 10 (2021), https://doi.org/10.1002/jev2.12081.

[8] S. Picciotto, M.E. Barone, D. Fierli, A. Aranyos, G. Adamo, D. Božič, D. P. Romancino, C. Stanly, R. Parkes, S. Morsbach, S. Raccosta, C. Paganini, A. Cusimano, V. Martorana, R. Noto, R. Carrotta, F. Librizzi, U. Capasso Palmiero, P. Santonicola, A. Iglič, M. Gai, L. Corcuera, A. Kisslinger, E. Di Schiavi, K. Landfester, G.L. Liguori, V. Kralj-Iglič, P. Arosio, G. Pocsfalvi, M. Manno, N. Touzet, A. Bongiovanni, Isolation of extracellular vesicles from microalgae: towards the production of sustainable and natural nanocarriers of bioactive compounds, Biomater. Sci. 9 (2021) 2917–2930, https://doi.org/10.1039/D0BM01696A.

[9] G. Adamo, P. Santonicola, S. Picciotto, P. Gargano, A. Nicosia, V. Longo, N. Aloi, D. P. Romancino, A. Paterna, E. Rao, S. Raccosta, R. Noto, M. Salamone, I. Deidda,

S. Costa, C. Di Sano, G. Zampi, S. Morsbach, K. Landfester, P. Colombo, M. Wei, P. Bergese, N. Touzet, M. Manno, E. Di Schiavi, A. Bongiovanni, Extracellular vesicles from the microalga *Tetraselmis chuii* are biocompatible and exhibit unique bone tropism along with antioxidant and anti-inflammatory properties, Commun. Biol. 7 (2024) 941, https://doi.org/10.1038/s42003-024-06612-9.

[10] T. Conlon, M. Schaaf, A. Mateos-Maroto, S. Picciotto, S. Morsbach, G. Adamo, S. Si, I. Lieberwirth, C. Rosenauer, K. Landfester, A. Bongiovanni, N. Touzet, Comparative effects of extracellular vesicles and liposomal nanocarriers on bleomycin-induced stress in A549 human adenocarcinoma cells, Biomed. Pharmacother. 187 (2025) 118081, https://doi.org/10.1016/j.biopha.2025.118081.

[11] C. Blanpain, Skin regeneration and repair, Nature 464 (2010) 686–687, https://doi.org/10.1038/464686a.

[12] M. Rinnerthaler, J. Bischof, M. Streubel, A. Trost, K. Richter, Oxidative stress in aging human skin, Biomolecules 5 (2015) 545–589, https://doi.org/10.3390/biom5020545.

[13] F. Solano, Photoprotection and skin pigmentation: melanin-related molecules and some other new agents obtained from natural sources, Molecules 25 (2020) 1537, https://doi.org/10.3390/molecules25071537.

[14] P.A. Riley, Melanin, Int. J. Biochem. Cell Biol. 29 (1997) 1235–1239, https://doi.org/10.1016/S1357-2725(97)00013-7.

[15] A. Salminen, K. Kaarniranta, A. Kauppinen, Photoaging: UV radiation-induced inflammation and immunosuppression accelerate the aging process in the skin, Inflamm. Res. 71 (2022) 817–831, https://doi.org/10.1007/s00011-022-01598-8.

[16] A. Sample, Y. He, Mechanisms and prevention of UV -induced melanoma, Photo Photo Photo 34 (2018) 13–24, https://doi.org/10.1111/phpp.12329.

[17] E. Fitsiou, T. Pulido, J. Campisi, F. Alimirah, M. Demaria, Cellular senescence and the senescence-associated secretory phenotype as drivers of skin photoaging, J. Invest. Dermatol. 141 (2021) 1119–1126, https://doi.org/10.1016/j.jid.2020.09.031.

[18] M.K. Kim, Y.C. Choi, S.H. Cho, J.S. Choi, Y.W. Cho, The antioxidant effect of small extracellular vesicles derived from aloe vera peels for wound healing, Tissue Eng. Regen. Med 18 (2021) 561–571, https://doi.org/10.1007/s13770-021-00367-8.

[19] M.D. Jelic, A.D. Mandic, S.M. Maricic, B.U. Srdjenovic, Oxidative stress and its role in cancer, J. Cancer Res. Ther. 17 (2021) 22–28, https://doi.org/10.4103/jcrt.JCRT_862_16.

[20] H. Yu, H. Feng, H. Zeng, Y. Wu, Q. Zhang, J. Yu, K. Hou, M. Wu, Exosomes: the emerging mechanisms and potential clinical applications in dermatology, Int. J. Biol. Sci. 20 (2024) 1778–1795, https://doi.org/10.7150/ijbs.92897.

[21] Y. Gu, J. Han, C. Jiang, Y. Zhang, Biomarkers, oxidative stress and autophagy in skin aging, Ageing Res. Rev. 59 (2020) 101036, https://doi.org/10.1016/j.arr.2020.101036.

[22] J. Chen, Y. Liu, Z. Zhao, J. Qiu, Oxidative stress in the skin: impact and related protection, Intern J. Cosmet. Sci. 43 (2021) 495–509, https://doi.org/10.1111/ics.12728.

[23] W.S. Jo, K.M. Yang, H.S. Park, G.Y. Kim, B.H. Nam, M.H. Jeong, Y.J. Choi, Effect of microalgal extracts of *Tetraselmis suecica* against UVB-induced photoaging in human skin fibroblasts, Toxicol. Res. 28 (2012) 241–248, https://doi.org/10.5487/TR.2012.28.4.241.

[24] S.Y. Kim, Y.M. Kwon, K.W. Kim, J.Y.H. Kim, Exploring the potential of Nannochloropsis sp. extract for cosmeceutical applications, Mar. Drugs 19 (2021) 690, https://doi.org/10.3390/md19120690.

[25] S. Picciotto, D. Belmonte, P. Gargano, G. Adamo, A. Paterna, E. Rao, T. Conlon, S. Raccosta, D.P. Romancino, G. Smeraldi, M. Salamone, N. Touzet, M. Manno, A. Bongiovanni, Optimizing sustainable production of high-quality microalgae-derived extracellular vesicles through batch-refeed perfusion cultivation, Journa Biotechnol. (2025), https://doi.org/10.1016/j.jbiotec.2025.07.016.

[26] C. Théry, K.W. Witwer, E. Aikawa, M.J. Alcaraz, J.D. Anderson, R. Andriantsitohaina, A. Antoniou, T. Arab, F. Archer, G.K. Atkin-Smith, D.C. Ayre, J.-M. Bach, D. Bachurski, H. Baharvand, L. Balaj, S. Baldacchino, N.N. Bauer, A.A. Baxter, M. Bebawy, C. Beckham, A. Bedina Zavec, A. Benmoussa, A.C. Berardi, P. Bergese, E. Bielska, C. Blenkiron, S. Bobis-Wozowicz, E. Boilard, W. Boireau, A. Bongiovanni, F.E. Borràs, S. Bosch, C.M. Boulanger, X. Breakefield, A.M. Breglio, M.Á. Brennan, D.R. Brigstock, A. Brisson, M.L. Broekman, J.F. Bromberg, P. Bryl-Górecka, S. Buch, A.H. Buck, D. Burger, S. Busatto, D. Buschmann, B. Bussolati, E.I. Buzás, J.B. Byrd, G. Camussi, D.R. Carter, S. Caruso, L.W. Chamley, Y.-T. Chang, C. Chen, S. Chen, L. Cheng, A.R. Chin, A. Clayton, S.P. Clerici, A. Cocks, E. Cocucci, R. J. Coffey, A. Cordeiro-da-Silva, Y. Couch, F.A. Coumans, B. Coyle, R. Crescitelli, M. F. Criado, C. D'Souza-Schorey, S. Das, A. Datta Chaudhuri, P. de Candia, E.F. De Santana, O. De Wever, H.A. del Portillo, T. Demaret, S. Deville, A. Devitt, B. Dhondt, D. Di Vizio, L.C. Dieterich, V. Dolo, A.P. Dominguez Rubio, M. Dominici, M.R. Dourado, T.A. Driedonks, F.V. Duarte, H.M. Duncan, R.M. Eichenberger, K. Ekström, S.E.L. Andaloussi, C. Elie-Caille, U. Erdbrügger, J.M. Falcón-Pérez, F. Fatima, J.E. Fish, M. Flores-Bellver, A. Försönits, A. Frelet-Barrand, F. Fricke, G. Fuhrmann, S. Gabrielsson, A. Gámez-Valero, C. Gardiner, K. Gärtner, R. Gaudin, Y. S. Gho, B. Giebel, C. Gilbert, M. Gimona, I. Giusti, D.C. Goberdhan, A. Görgens, S. M. Gorski, D.W. Greening, J.C. Gross, A. Gualerzi, G.N. Gupta, D. Gustafson, A. Handberg, R.A. Haraszti, P. Harrison, H. Hegyesi, A. Hendrix, A.F. Hill, F.H. Hochberg, K.F. Hoffmann, B. Holder, H. Holthofer, B. Hosseinkhani, G. Hu, Y. Huang, V. Huber, S. Hunt, A.G.-E. Ibrahim, T. Ikezu, J.M. Inal, M. Isin, A. Ivanova, H.K. Jackson, S. Jacobsen, S.M. Jay, M. Jayachandran, G. Jenster, L. Jiang, S.M. Johnson, J.C. Jones, A. Jong, T. Jovanovic-Talisman, S. Jung, R. Kalluri, S. Kano, S. Kaur, Y. Kawamura, E.T. Keller, D. Khamari, E. Khomyakova, A. Khvorova, P. Kierulf, K.P. Kim, T. Kislinger, M. Klingeborn, D.J. Klinke, M. Kornek, M.M. Kosanović, Á.F. Kovács, E.-M. Krämer-Albers, S. Krasemann, M. Krause, I.V. Kurochkin, G.D. Kusuma, S. Kuypers, S. Laitinen, S.M. Langevin, L.R. Languino, J. Lannigan, C. Lässer, L.C. Laurent, G. Lavieu, E. Lázaro-Ibáñez, S. Le Lay, M.-S. Lee, Y.X.F. Lee, D.S. Lemos, M. Lenassi, A. Leszczynska, I.T. Li, K. Liao, S.F. Libregts, E. Ligeti, R. Lim, S.K. Lim, A. Linē, K. Linnemannstöns, A. Llorente, C.A. Lombard, M. J. Lorenowicz, Á.M. Lörincz, J. Lötvall, J. Lovett, M.C. Lowry, X. Loyer, Q. Lu, B. Lukomska, T.R. Lunavat, S.L. Maas, H. Malhi, A. Marcilla, J. Mariani, J. Mariscal, E.S. Martens-Uzunova, L. Martin-Jaular, M.C. Martinez, V.R. Martins, M. Mathieu, S. Mathivanan, M. Maugeri, L.K. McGinnis, M.J. McVey, D.G. Meckes, K.L. Meehan, I. Mertens, V.R. Minciacchi, A. Möller, M. Møller Jørgensen, A. Morales-Kastresana, J. Morhayim, F. Mullier, M. Muraca, L. Musante, V. Mussack, D.C. Muth, K.H. Myburgh, T. Najrana, M. Nawaz, I. Nazarenko, P. Nejsum, C. Neri, T. Neri, R. Nieuwland, L. Nimrichter, J.P. Nolan, E.N. Nolte-'t Hoen, N. Noren Hooten, L. O'Driscoll, T. O'Grady, A. O'Loghlen, T. Ochiya, M. Olivier, A. Ortiz, L.A. Ortiz, X. Osteikoetxea, O. Østergaard, M. Ostrowski, J. Park, D.M. Pegtel, H. Peinado, F. Perut, M.W. Pfaffl, D.G. Phinney, B.C. Pieters, R.C. Pink, D.S. Pisetsky, E. Pogge von Strandmann, I. Polakovicova, I.K. Poon, B.H. Powell, I. Prada, L. Pulliam, P. Quesenberry, A. Radeghieri, R.L. Raffai, S. Raimondo, J. Rak, M.I. Ramirez, G. Raposo, M.S. Rayyan, N. Regev-Rudzki, F.L. Ricklefs, P.D. Robbins, D.D. Roberts, S. C. Rodrigues, E. Rohde, S. Rome, K.M. Rouschop, A. Rughetti, A.E. Russell, P. Saá, S. Sahoo, E. Salas-Huenuleo, C. Sánchez, J.A. Saugstad, M.J. Saul, R.M. Schiffelers, R. Schneider, T.H. Schøyen, A. Scott, E. Shahaj, S. Sharma, O. Shatnyeva, F. Shekari, G.V. Shelke, A.K. Shetty, K. Shiba, P.R.-M. Siljander, A.M. Silva, A. Skowronek, O.L. Snyder, R.P. Soares, B.W. Sódar, C. Soekmadji, J. Sotillo, P.D. Stahl, W. Stoorvogel, S.L. Stott, E.F. Strasser, S. Swift, H. Tahara, M. Tewari, K. Timms, S. Tiwari, R. Tixeira, M. Tkach, W.S. Toh, R. Tomasini, A.C. Torrecilhas, J. P. Tosar, V. Toxavidis, L. Urbanelli, P. Vader, B.W. van Balkom, S.G. van der Grein, J. Van Deun, M.J. van Herwijnen, K. Van Keuren-Jensen, G. van Niel, M.E. van Royen, A.J. van Wijnen, M.H. Vasconcelos, I.J. Vechetti, T.D. Veit, L.J. Vella, É. Velot, F.J. Verweij, B. Vestad, J.L. Viñas, T. Visnovitz, K.V. Vukman, J. Wahlgren, D.C. Watson, M.H. Wauben, A. Weaver, J.P. Webber, V. Weber, A.M. Wehman, D.J. Weiss, J.A. Welsh, S. Wendt, A.M. Wheelock, Z. Wiener, L. Witte, J. Wolfram, A. Xagorari, P. Xander, J. Xu, X. Yan, M. Yáñez-Mó, H. Yin, Y. Yuana, V. Zappulli, J. Zarubova, V. Žėkas, J. Zhang, Z. Zhao, L. Zheng, A.R. Zheutlin, A.M. Zickler, P. Zimmermann, A.M. Zivkovic, D. Zocco, E.K. Zuba-Surma, Minimal information for studies of extracellular vesicles 2018 (MISEV2018): a position statement of the International Society for Extracellular Vesicles and update of the MISEV2014 guidelines, Journal of Extracellular Vesicles 7 (2018) 1535750. https://doi.org/10.1080/20013078.2018.1535750.

[27] G. Adamo, S. Picciotto, P. Gargano, A. Paterna, S. Raccosta, E. Rao, D. P. Romancino, G. Ghersi, M. Manno, M. Salamone, A. Bongiovanni, DetectEV: a functional enzymatic assay to assess integrity and bioactivity of extracellular vesicles, J. Extracell. Vesicle 14 (2025), https://doi.org/10.1002/jev2.70030.

[28] F. Loria, S. Picciotto, G. Adamo, A. Zendrini, S. Raccosta, M. Manno, P. Bergese, G. L. Liguori, A. Bongiovanni, N. Zarovni, A decision-making tool for navigating extracellular vesicle research and product development, J. Extracell. Vesicle 13 (2024) e70021, https://doi.org/10.1002/jev2.70021.

[29] J.H. Kim, J. Lee, J. Park, Y.S. Gho, Gram-negative and Gram-positive bacterial extracellular vesicles, Semin. Cell Dev. Biol. 40 (2015) 97–104, https://doi.org/10.1016/j.semcdb.2015.02.006.

[30] S. Picciotto, P. Santonicola, A. Paterna, E. Rao, S. Raccosta, D.P. Romancino, R. Noto, N. Touzet, M. Manno, E. Di Schiavi, A. Bongiovanni, G. Adamo, Extracellular vesicles from microalgae: uptake studies in human cells and Caenorhabditis elegans, Front. Bioeng. Biotechnol. 10 (2022) 830189, https://doi.org/10.3389/fbioe.2022.830189.

[31] D.F. Basri, L.C. Lew, R.V. Muralitharan, T.S. Nagapan, A.R. Ghazali, Pterostilbene inhibits the melanogenesis activity in UVB-irradiated B164A5 cells, Dose Response 19 (2021) 15593258211047651, https://doi.org/10.1177/15593258211047651.

[32] N. Shimoda, Y. Mutou, N. Shimura, M. Tsukimoto, A. Awaya, S. Kojima, Effect of heterocyclic pyrimidine compounds on UVB-induced cell damage in human keratinocytes and on melanogenesis in mouse B16 cells, Biol. Pharm. Bull. 33 (2010) 862–868, https://doi.org/10.1248/bpb.33.862.

[33] R. Lee, H.J. Ko, K. Kim, Y. Sohn, S.Y. Min, J.A. Kim, D. Na, J.H. Yeon, Anti-melanogenic effects of extracellular vesicles derived from plant leaves and stems in mouse melanoma cells and human healthy skin, J. Extracell. Vesicle 9 (2020) 1703480, https://doi.org/10.1080/20013078.2019.1703480.

[34] L. Chen, Y. Hu, M. Zhang, L. Liu, J. Ma, Z. Xu, J. Zhang, H. Gu, K. Chen, METTL14 affects UVB -induced human dermal fibroblasts photoaging via miR -100-3p biogenesis in an m^6 A -dependent manner, Aging Cell 23 (2024) e14123, https://doi.org/10.1111/acel.14123.

[35] A.Y. Park, J. Lee, Y. Jang, Y.-J. Kim, J. Lee, S.-Y. Kim, B. Kim, K. Yoo, Exosomes derived from human dermal fibroblasts protect against UVB-induced skin photoaging, Int. J. Mol. Med 52 (2023) 120, https://doi.org/10.3892/ijmm.2023.5323.

[36] H.-J. Shin, C.T. Oh, T.-R. Kwon, H.S. Beak, Y.H. Joo, J.-H. Kim, C.S. Lee, J.H. Lee, B.J. Kim, S.S. Shin, E.-S. Park, A novel adamantyl benzylbenzamide derivative, AP736, inhibits melanogenesis in B16F10 mouse melanoma cells via glycogen synthase kinase 3β phosphorylation, Int. J. Mol. Med. 36 (2015) 1353–1360, https://doi.org/10.3892/ijmm.2015.2348.

[37] A. Paterna, E. Rao, G. Adamo, S. Raccosta, S. Picciotto, D. Romancino, R. Noto, N. Touzet, A. Bongiovanni, M. Manno, Isolation of extracellular vesicles from microalgae: a renewable and scalable bioprocess, Front. Bioeng. Biotechnol. 10 (2022) 836747, https://doi.org/10.3389/fbioe.2022.836747.

[38] E.D. Sverdlov, Amedeo Avogadro's cry: what is 1 μg of exosomes? Bioessays 34 (2012) 873–875, https://doi.org/10.1002/bies.201200045.

[39] N. Coulombier, T. Jauffrais, N. Lebouvier, Antioxidant compounds from microalgae: a review, Mar. Drugs 19 (2021) 549, https://doi.org/10.3390/md19100549.

[40] C. Sansone, C. Galasso, I. Orefice, G. Nuzzo, E. Luongo, A. Cutignano, G. Romano, C. Brunet, A. Fontana, F. Esposito, A. Ianora, The green microalga *Tetraselmis suecica* reduces oxidative stress and induces repairing mechanisms in human cells, Sci. Rep. 7 (2017), https://doi.org/10.1038/srep41215.
[41] D.E. Heck, A.M. Vetrano, T.M. Mariano, J.D. Laskin, UVB light stimulates production of reactive oxygen species, J. Biol. Chem. 278 (2003) 22432–22436, https://doi.org/10.1074/jbc.C300048200.
[42] L. Subedi, T.H. Lee, H.M. Wahedi, S.-H. Baek, S.Y. Kim, Resveratrol-enriched rice attenuates UVB-ROS-induced skin aging via downregulation of inflammatory cascades, Oxid. Med. Cell. Longev. 2017 (2017) 8379539, https://doi.org/10.1155/2017/8379539.
[43] Y.C. Boo, Arbutin as a skin depigmenting agent with antimelanogenic and antioxidant properties, Antioxidants 10 (2021) 1129, https://doi.org/10.3390/antiox10071129.
[44] J. Takebayashi, R. Ishii, J. Chen, T. Matsumoto, Y. Ishimi, A. Tai, Reassessment of antioxidant activity of arbutin: multifaceted evaluation using five antioxidant assay systems, Free Radic. Res. 44 (2010) 473–478, https://doi.org/10.3109/10715761003610760.
[45] F. Lu, Q. Zhou, M. Liang, H. Liang, Y. Yu, Y. Li, Y. Zhang, L. Lu, Y. Zheng, J. Hao, P. Shu, J. Liu, α-Arbutin ameliorates UVA-induced photoaging through regulation of the SIRT3/PGC-1α pathway, Front. Pharm. 15 (2024) 1413530, https://doi.org/10.3389/fphar.2024.1413530.
[46] Ç. Yarkent, C. Gürlek, S.S. Oncel, Potential of microalgal compounds in trending natural cosmetics: a review, Sustain. Chem. Pharm. 17 (2020) 100304, https://doi.org/10.1016/j.scp.2020.100304.
[47] R.R. Ambati, D. Gogisetty, R.G. Aswathanarayana, S. Ravi, P.N. Bikkina, L. Bo, S. Yuepeng, Industrial potential of carotenoid pigments from microalgae: current trends and future prospects, Crit. Rev. Food Sci. Nutr. 59 (2019) 1880–1902, https://doi.org/10.1080/10408398.2018.1432561.
[48] B. Santiesteban-Romero, M. Martínez-Ruiz, J.E. Sosa-Hernández, R. Parra-Saldívar, H.M.N. Iqbal, Microalgae photo-protectants and related bio-carriers loaded with bioactive entities for skin applications—an insight of microalgae biotechnology, Mar. Drugs 20 (2022) 487, https://doi.org/10.3390/md20080487.
[49] N. Rosic, Unveiling the anti-aging potential of marine natural bioproducts, Mar. Drugs 23 (2025) 165, https://doi.org/10.3390/md23040165.
[50] A. Najafi, M. Heidary, R.M. Martinez, A.R. Baby, M.H. Morowvat, Microalgae-based sunscreens as green and sustainable cosmetic products, Intern J. Cosmet. Sci. 47 (2025) 213–222, https://doi.org/10.1111/ics.13019.
[51] S.G.M. Lima, M.C.L.C. Freire, V.D.S. Oliveira, C. Solisio, A. Converti, Á.A.N. De Lima, Astaxanthin delivery systems for skin application: a review, Mar. Drugs 19 (2021) 511, https://doi.org/10.3390/md19090511.
[52] M. Mourelle, C. Gómez, J. Legido, The potential use of marine microalgae and cyanobacteria in cosmetics and thalassotherapy, Cosmetics 4 (2017) 46, https://doi.org/10.3390/cosmetics4040046.
[53] M.V. Vieira, L.M. Pastrana, P. Fuciños, Microalgae encapsulation systems for food, pharmaceutical and cosmetics applications, Mar. Drugs 18 (2020) 644, https://doi.org/10.3390/md18120644.
[54] S.Y. Koo, I.-K. Mok, C.-H. Pan, S.M. Kim, Preparation of fucoxanthin-loaded nanoparticles composed of casein and chitosan with improved fucoxanthin bioavailability, J. Agric. Food Chem. 64 (2016) 9428–9435, https://doi.org/10.1021/acs.jafc.6b04376.
[55] S. Mota, L. Rego, E. Sousa, M.T. Cruz, I.M.D. Almeida, Usage frequency and ecotoxicity of skin depigmenting agents, Pharmaceuticals 18 (2025) 368, https://doi.org/10.3390/ph18030368.
[56] W. Westerhof, T.J. Kooyers, Hydroquinone and its analogues in dermatology – a potential health risk, J. Cosmet. Dermatol. 4 (2005) 55–59, https://doi.org/10.1111/j.1473-2165.2005.40202.x.
[57] M. Nakagawa, K. Kawai, K. Kawai, Contact allergy to kojic acid in skin care products, Contact Dermat. 32 (1995) 9–13, https://doi.org/10.1111/j.1600-0536.1995.tb00832.x.
[58] SCCS (Scientific Committee on Consumer Safety), Opinion on the safety of alpha-(CAS No. 84380–018, EC No. 617–561-8) and beta-arbutin (CAS No. 497–76-7, EC No. 207–8503) in cosmetic products, (n.d.). https://health.ec.europa.eu/publications/safety-alpha-arbutin-and-beta-arbutin-cosmetic-products_en.
[59] H. Kim, H.-R. Choi, D.-S. Kim, K.-C. Park, Topical hypopigmenting agents for pigmentary disorders and their mechanisms of action, Ann. Dermatol. 24 (1) (2012), https://doi.org/10.5021/ad.2012.24.1.1.
[60] G.-W. Oh, S.-C. Ko, S.-Y. Heo, V.-T. Nguyen, G. Kim, C.H. Jang, W.S. Park, I.-W. Choi, Z.-J. Qian, W.-K. Jung, A novel peptide purified from the fermented microalga Pavlova lutheri attenuates oxidative stress and melanogenesis in B16F10 melanoma cells, Process Biochem. 50 (2015) 1318–1326, https://doi.org/10.1016/j.procbio.2015.05.007.
[61] R. Favas, J. Morone, R. Martins, V. Vasconcelos, G. Lopes, Cyanobacteria and microalgae bioactive compounds in skin-ageing: potential to restore extracellular matrix filling and overcome hyperpigmentation, J. Enzym. Inhib. Med. Chem. 36 (2021) 1829–1838, https://doi.org/10.1080/14756366.2021.1960830.